

Magneto-optical Trap for Polar Molecules

Benjamin K. Stuhl,* Brian C. Sawyer, Dajun Wang, and Jun Ye

*JILA, National Institute of Standards and Technology and the University of Colorado
Department of Physics, University of Colorado, Boulder, Colorado 80309-0440, USA*

(Received 14 August 2008; published 9 December 2008)

We propose a method for laser cooling and trapping a substantial class of polar molecules and, in particular, titanium (II) oxide (TiO). This method uses pulsed electric fields to nonadiabatically remix the ground-state magnetic sublevels of the molecule, allowing one to build a magneto-optical trap based on a quascycling $J' = J'' - 1$ transition. Monte Carlo simulations of this electrostatically remixed magneto-optical trap demonstrate the feasibility of cooling TiO to a temperature of 10 μK and trapping it with a radiation-pumping-limited lifetime on the order of 80 ms.

DOI: 10.1103/PhysRevLett.101.243002

PACS numbers: 37.10.Pq, 37.10.Mn, 37.10.Vz

The field of ultracold polar molecules has recently made great strides. Coherent optical transfer of magnetoassociated molecules can now produce ultracold molecular gases in the $X^1\Sigma$ ($v = 0$) ground state with densities of 10^{12} cm^{-3} and translational temperatures of 350 nK [1]. Incoherent photoassociation techniques can reach the $X^1\Sigma$ ($v = 0$) ground state at 100 μK [2]. With these temperatures and the reasonably large electric dipole moments available from heteronuclear bialkali molecules [e.g., 0.76 D for $X^1\Sigma$ ($v = 0$) K Rb [3]], progress towards quantum simulations of condensed matter systems [4,5] and quantum computation [6,7] should be rapid. In fields such as ultracold chemistry [8], access to molecular species beyond the bialkali family is of great interest. Arbitrary species can be cooled to the kelvin regime through buffer-gas cooling [9,10], while Stark deceleration [11,12] reaches the tens of millikelvin level for selected light molecules. Unfortunately, there is no demonstrated technique to further compress and cool the lukewarm molecular clouds resulting from the latter two techniques. Even cavity-mediated schemes for molecular laser cooling [13–16], while in the abstract highly attractive methods for cooling a broad, chemically interesting set of molecules, have so far been unable to cool these lukewarm samples, due to the schemes' low scattering rates [15], small cavity mode volumes [16], and requirement of multiparticle collective effects [13,14].

Direct, free-space laser cooling and trapping would be the ideal method for producing ultracold molecules, just as it is for atoms. Unfortunately, atoms are, in general, much easier to laser cool than molecules, due to the latter's glaring lack of cycling transitions. Laser cooling generally requires electronic transitions, as vibrational and rotational transitions have impractically long excited-state lifetimes unless a cavity is used [16]. Unfortunately, these “electronic” transitions are never purely electronic. Rather, they are rovibronic and decay into various rotational, vibrational, or hyperfine excited states, as well as the original ground state [17].

The branching ratios of these rovibronic decays, however, are governed by the molecular structure and the dipole selection rules. This implies that a clever choice of molecule can greatly reduce the number of possible decays. Decays into excited hyperfine states are impossible in molecules with zero nuclear spin, as these molecules have no hyperfine structure. The Franck-Condon ratios for decay back to the ground vibrational level can be quite good (99+% for selected molecules [18]). However, the only constraint on decays to rotationally excited levels is that all decays satisfy the total angular momentum selection rule $\Delta J = 0, \pm 1$ [11]. Thus, even without hyperfine structure, it may take up to three lasers per vibrational level to repump the three possible rotational decays. However, if the ground-state angular momentum J'' is greater than the excited-state angular momentum J' , two of these three decays are forbidden. In this case, the molecule *must* follow the angular momentum cycle $J'' \rightarrow J' = J'' - 1 \rightarrow J''$, and so only one laser is required per relevant vibrational level—making laser cooling of these molecules truly practical.

Thus, by combining these various transition closure criteria, we can identify a class of molecules that are exceptionally good candidates for laser cooling: They have no net nuclear spin and good Franck-Condon overlaps, and their ground or lowest metastable state has a higher angular momentum than the first accessible electronically excited state. For nonsinglet molecules, the excited electronic level must also not be a Σ state, as the lack of spin-orbit splitting in Σ states means that the excited state can decay across the spin-orbit ladder.

We have identified a number of molecules that satisfy all of the above requirements. TiO and TiS are both satisfactory in their absolute ground states. Metastable FeC, ZrO, HfO, ThO, SeO, and the like are promising [19]. We expect that some other, as-yet uncharacterized metal oxides, sulfides, and carbides should also have the necessary electronic structure. If one is willing to accept some hyperfine structure as the price of chemical diversity, some metal

hydrides and metal halides may provide additional suitable candidates.

Of these candidates, we chose to focus on TiO, due to its viability in its absolute ground state and the breadth of spectroscopy and theory available in the literature [20–28]. A simplified level structure of TiO is shown in Fig. 1. The lowest ground state of TiO is the $X^3\Delta_1$, with spin-orbit constant $A^{(X^3\Delta)} = 50.61 \text{ cm}^{-1}$ and rotational constant $B^{(X^3\Delta)} = 0.534 \text{ cm}^{-1}$ [28]. The lowest excited state is the $E^3\Pi_0$, with $A^{(E^3\Pi)} = 86.82 \text{ cm}^{-1}$ and $B^{(E^3\Pi)} = 0.515 \text{ cm}^{-1}$ [23]. (While the $d^1\Sigma^+$ and $a^1\Delta$ levels are energetically below the $E^3\Pi$ level, the intersystem branching ratio is expected to be very small.) As Fig. 1 shows, the Franck-Condon factors [20,21] for the $E^3\Pi - X^3\Delta$ band are quite favorable, yielding a population leak of 3×10^{-4} scatter $^{-1}$ (or a mean of ~ 3300 scatters before going into a dark state) with two repump lasers. The laser wavelengths, saturation intensities (I_{sat}), and Franck-Condon factors for the cooling and repump lines are summarized in Table I. Note that these transitions are all accessible with diode lasers. The saturation intensities are extremely low, as the natural linewidth γ of the $E^3\Pi - X^3\Delta$ transition is on the order of $2\pi \times 32\text{--}40 \text{ kHz}$ [24,25]. This is about 5 times weaker than the intercombination line used to build a Yb magneto-optical trap (MOT) in [29]. However, with the use of a cryogenic buffer-gas-cooled TiO source (similar to [30]), the scattering rate is still large enough to work with.

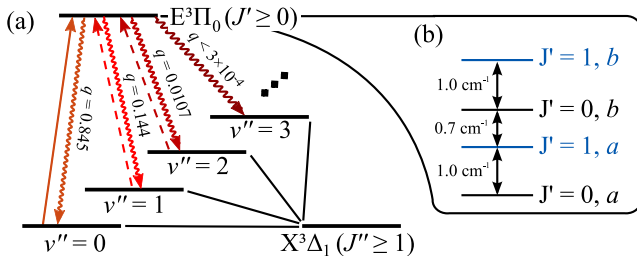


FIG. 1 (color online). (not to scale) (a) The electronic level structure of TiO and the transitions of interest for laser cooling. The $X^3\Delta$ ground state is split by the spin-orbit interaction into the three $X^3\Delta_{1-3}$ sublevels, of which the $X^3\Delta_1$ level is the lowest. Each sublevel contains a vibrational ladder, while each vibrational level contains a ladder of rotationally excited states (not shown). $^{48}\text{Ti}^{16}\text{O}$ has zero nuclear spin, and thus there is no hyperfine structure. The ground-state Λ doublet (not shown) is much less than the natural linewidth of the $E^3\Pi \leftarrow X^3\Delta$ transition. The solid arrow denotes the $v' = 0 \leftarrow v'' = 0$ $P(1)$ -branch cooling laser, and the dashed arrows denote the $v' = 0 \leftarrow v'' = 1$ and $v' = 0 \leftarrow v'' = 2$ $P(1)$ -branch repump lasers. The squiggly lines depict the dipole-allowed decays, with the associated Franck-Condon factor q [20] next to each decay. (b) The rotational and Λ -doublet structure of the $E^3\Pi_0$ electronic excited manifold. The states are interleaved, as the rotational splitting is smaller than the Λ -doublet splitting; a and b denote the parity states. Both the cooling and repump lasers address the $J' = 0, a$ state.

The prospect of building a TiO MOT is tantalizing, given this quasiclosed transition. Traditional MOTs work using a $J' = J'' + 1$ transition and a magnetic field to break the degeneracy between the excited-state magnetic sublevels. The MOT beams are polarized so that the local orientation and strength of the quadrupole magnetic field cause the atom to preferentially scatter from the laser beam providing a position-dependent restoring force and a velocity-dependent damping force. The fact that $J' > J''$ means that the atom can always scatter from the correct beam, as shown in Fig. 2(a). However, the standard MOT will not work for molecules using the aforementioned $J' = J'' - 1$ transition [Fig. 2(b)]. While a magnetic field can break the degeneracy of the ground-state magnetic sublevels and thus provide beam selectivity, the $|m_{J''}| = J''$ stretched states are effectively dark states, as they can interact with only one of the laser beams, not both [31].

What is needed, then, is a way to continually remix the ground-state sublevels so that all of the molecules spend some fraction of their time in bright states. Fortunately, polar molecules provide just the handle needed to accomplish this: The effective magnetic (B) and electric (E) moments of a polar molecule depend in different ways on m_J . Thus, applying a sudden (i.e., nonadiabatic) electric field orthogonal (or at least nonparallel) to the local magnetic field reprojects the total angular momentum against a new axis, randomizing m_J (and the Λ -doublet state) by coupling the two Λ -doublet manifolds together. At high remix rates and high laser saturations, the molecules' time is equally divided across the $2(2J'' + 1)$ ground and $2J' + 1$ excited states (the factor of 2 in the ground state is due to the electrostatic mixing of the Λ doublet), but they can decay only while they are in an excited state. Thus, while the molecules are effectively always bright, the maximum photon scattering rate is only $\frac{2J'+1}{2(2J''+1)+(2J'+1)}\gamma$. Such remixing of the ground-state magnetic sublevels allows the building of a new kind of trap, the electrostatically remixed magneto-optical trap (ER-MOT). The ER-MOT operation is shown in Fig. 2(b). Note that, as the local direction of the quadrupole B field spans all of 4π steradians over the MOT volume, a single E -field pulse will be parallel to the local B field in some region and therefore ineffective at remixing the m_J 's there. This hole can, however, easily be closed by

TABLE I. The wavelengths, Franck-Condon factors, and saturation intensities of the cooling and repump transitions of TiO.

v''	$\lambda_{0,v''}$ [nm]	Franck-Condon factor $q_{0,v''}^a$	Estimated I_{sat} [$\mu\text{W}/\text{cm}^2$] ^b
0	844.7227 [23]	0.845; 0.872 [21]	8
1	923 ^c	0.144	48
2	1017 ^c	0.0107	645

^aFrom Ref. [20], except for the second value of q_{00} .

^bEstimated for a two-level system with $\gamma = 2\pi \times 32 \text{ kHz}$ and scaled by $1/q_{0v''}$.

^cCalculated using the diatomic molecular constants of [22].

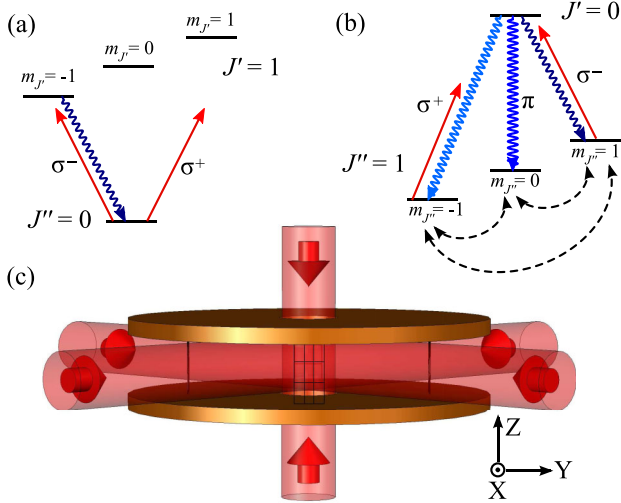


FIG. 2 (color online). (a) The level structure of a traditional MOT. The local magnetic field strength and orientation combined with the Doppler shift enhance the scattering from the laser beam that provides the damping and restoring forces and suppresses scattering from the counterpropagating beam. Since $J' > J''$, the ground state(s) are always able to scatter from every beam. (b) The level structure of the ER-MOT. The local magnetic field still governs which laser is preferentially scattered, but angular momentum conservation forbids some ground states from interacting with the preferred beam. To overcome this, the ground-state magnetic sublevel populations are remixed by pulsed electric fields, as represented by the dashed lines. (c) A sample ER-MOT design. A pair of electromagnet coils are aligned in anti-Helmholtz fashion to produce a quadrupole field. Six beams of the cooling laser are converged on the center with their polarizations oriented as usual for a MOT, but a set of four open-mesh grids are added. The grids are pulsed in pairs (e.g., first the X -axis pair and then the Y -axis pair) to produce the dipole electric fields needed to remix the magnetic sublevels. The center is also illuminated by the repump lasers (not shown).

applying a second E -field pulse, nonparallel to the first. A basic ER-MOT design is shown in Fig. 2(c).

To build an ER-MOT with TiO, there is a minor technical complication. To leading order, the molecular magnetic moment can be written as $\mu = \mu_B m_J (g_L \Lambda + g_S \Sigma) \frac{\Omega}{J(J+1)}$. Since $g_L \approx 1$ and $g_S \approx 2$, the magnetic moment of the $X^3\Delta_1$ ($\Lambda = 2$ and $\Sigma = -1$) state is small, likely on the order of $\alpha \mu_B$, or the fine-structure constant times the Bohr magneton. In contrast, while $\Omega = 0$ in the $E^3\Pi_0$ state, the large Λ -doublet splitting indicates strong mixing with higher electronic excited states, and so by analogy with the $B^3\Pi_0$ optical Zeeman measurements of Ref. [32], we estimate the magnetic moment to be ~ 10 times that of the $X^3\Delta_1$. This, combined with the narrowness of the $E^3\Pi \leftrightarrow X^3\Delta$ transition, implies that the dynamics of a TiO ER-MOT will have more in common with narrow-line alkaline-earth MOTs [33] than normal alkali metal MOTs. Given these predicted magnetic moments, the magnetic gradient in a TiO ER-MOT must be $\lesssim 100$ G/cm. This gradient can be easily achieved with water-cooled electromagnets [12]

or rare-earth permanent magnets [34]. In contrast, the large (≈ 3 Debye [27]) electric dipole moment of TiO and its extremely small ground-state Λ -doublet spacing [26] mean that electric fields of only 1 V/cm will give Stark shifts of about 50γ —far more than the Zeeman shift within the ER-MOT and thus sufficient to reproject m_J . These small fields can easily be switched with rise times on the order of 10 ns (a frequency of 2800γ and 56 times the Larmor frequency due to the electric field), and thus nonadiabaticity is assured.

A final concern regarding the viability of the TiO ER-MOT is that either the electrostatic or the magnetic fields might somehow cause population loss by mixing in rotationally excited $J' > 0$ states, which could then decay to $J'' > 1$ states and be lost. Fortunately, this loss is inhibited by the ~ 1 cm $^{-1}$ rotational splitting [Fig. 1(b)]. Neither the Zeeman nor the Stark shifts within the ER-MOT are anticipated to be larger than ~ 100 MHz, and so the perturbative probability to leave the desired $J' = 0$ state is $(\frac{100 \text{ MHz}}{30 \text{ GHz}})^2 \approx 10^{-5}$. This is much smaller than the 3×10^{-4} scatter $^{-1}$ loss rate from decays to $v'' \geq 3$ and so is of no importance.

To verify the feasibility of building an ER-MOT with TiO, we performed a set of 3D semiclassical Monte Carlo simulations. We conservatively assumed a natural line-width of $\gamma = 2\pi \times 32$ kHz, a magnetic dipole moment of $\alpha \mu_B$, and an electric dipole moment of 3 D. We used a $1/e^2$ laser waist diameter of 6 cm. Our code treated photon scattering and molecule kinematics semiclassically and approximated the electrostatic remixing as a sudden reprojected of the diagonalized Zeeman Hamiltonian wave function against a new Stark plus Zeeman Hamiltonian. In addition, the simulations used a set of 60 additional red-detuned frequency components (4.1γ spacing, 7.8 MHz total bandwidth) within the cooling beams to increase the capture velocity of the ER-MOT, similar to the approach used in the Yb MOT of Ref. [29]. For ease of simulation, we used a discrete molecular packet rather than a continuous source. The packet was a 3 mm sphere initially centered at -4.2 cm on the X axis in the coordinate system of Fig. 2(c). It had a flat velocity distribution of 8 ± 3.5 m/s centered in orientation around \hat{x} , with an opening half-angle of 0.3 rad. The magnetic field gradient was 51 G/cm, and the electric field was pulsed to 4 V/cm for 100 ns at a rate of 50 kHz. The cooling laser was detuned by 3.5γ to the red, with a saturation parameter of $s_{\text{cool}} = 10.5$ per frequency component. The repump lasers had saturations $s_{\text{repump}} = 6.1$.

These simulation parameters yield the loading and temperature curves shown in Figs. 3(a) and 3(b), respectively. The final temperature was approximately 10 μ K. The ER-MOT lifetime was limited to about 80 ms by radiation pumping into vibrationally excited dark states. The estimated capture velocity was 5.7 m/s, which when taking the rotational distribution into account allows the capture of about 0.02% of a 4.2 K thermal distribution. If one

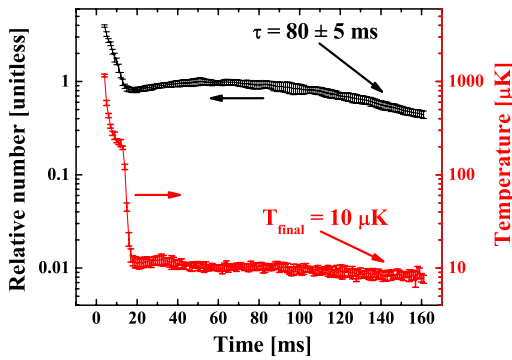


FIG. 3 (color online). Number (upper, black) and temperature (lower, red) time-of-flight plots for the loading of a molecular packet into a simulated TiO ER-MOT. The initial spike on the number plot is the molecular packet flying through the ER-MOT volume; the broad hump is the actual captured molecules. The decay of the molecule number is due to radiation pumping of the captured population into excited $v'' \geq 3$ levels and yields an ER-MOT lifetime of 80 ± 5 ms. Error bars represent statistics over multiple simulation runs.

assumes a 4.2 K source flux of 10^{10} s^{-1} [30], the calculated capture velocity, lifetime, and ER-MOT radius predict an ER-MOT number of 10^5 and a density of 10^9 cm^{-3} .

In addition, we studied the importance of the electrostatic remixing to the ER-MOT operation. Figure 4 plots the molecule number after 160 ms against the electrostatic remix frequency Γ_{remix} . The plot clearly shows the importance of the electrostatic remixing. At $\Gamma_{\text{remix}} \ll \frac{\gamma}{2\pi}$, no molecules are captured, since the molecules are optically pumped out of the bright state much faster than they are remixing back into it. For $\Gamma_{\text{remix}} \approx \frac{\gamma}{2\pi}$, the capture efficiency rises with increasing Γ_{remix} , and then the efficiency saturates around $\Gamma_{\text{remix}} = \frac{\gamma}{2\pi}$, as the molecules become evenly divided among the various ground sublevels. As additional validation checks on the simulation code, we verified that turning off the repump lasers does indeed inhibit the formation of an ER-MOT by pumping the entire population into vibrationally excited states. We also verified that we could reproduce the experimental Yb MOT of

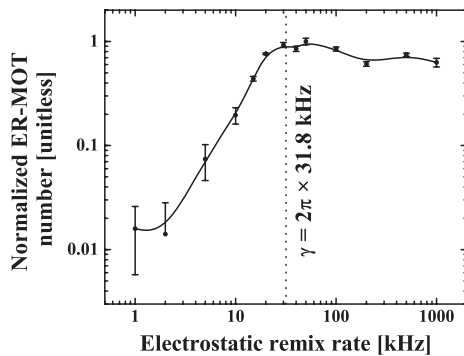


FIG. 4. Fractional capture vs electrostatic remix rate after 160 ms of simulation time for the TiO ER-MOT. Error bars represent statistics over multiple simulation runs. The curve is only a guide to the eye.

Ref. [29] by modifying the code to simulate a $J' = J'' + 1$ setup with the correct atomic parameters.

In summary, we have shown that molecules whose lowest ground- or metastable level-intersecting electronic transition has $J' = J'' - 1$ constitute good candidates for direct laser cooling. We have found several molecules that satisfy this requirement and have no hyperfine structure. We have proposed a method to use the electric dipole moment of these molecules to remove dark states in the ground and thus build an electrostatically remixed magneto-optical trap. We have validated these ideas through Monte Carlo simulation for a specific molecule (TiO) and verified the necessity and efficacy of the electrostatic remixing.

We thank M. Yeo, E. Hudson, and D. DeMille for valuable discussions and thank NIST, DOE, and NSF for support.

*stuhl@jila.colorado.edu

- [1] K.-K. Ni *et al.*, *Science* **322**, 231 (2008).
- [2] J. M. Sage *et al.*, *Phys. Rev. Lett.* **94**, 203001 (2005).
- [3] S. Kotochigova *et al.*, *Phys. Rev. A* **68**, 022501 (2003).
- [4] K. Göral *et al.*, *Phys. Rev. Lett.* **88**, 170406 (2002).
- [5] A. Micheli *et al.*, *Nature Phys.* **2**, 341 (2006).
- [6] D. DeMille, *Phys. Rev. Lett.* **88**, 067901 (2002).
- [7] C. Lee and E. A. Ostrovskaya, *Phys. Rev. A* **72**, 062321 (2005).
- [8] E. R. Hudson *et al.*, *Phys. Rev. A* **73**, 063404 (2006); R. V. Krems, *Phys. Chem. Chem. Phys.* **10**, 4079 (2008).
- [9] J. D. Weinstein *et al.*, *Nature (London)* **395**, 148 (1998).
- [10] W. C. Campbell *et al.*, *Phys. Rev. Lett.* **98**, 213001 (2007).
- [11] H. L. Bethlem and G. Meijer, *Int. Rev. Phys. Chem.* **22**, 73 (2003).
- [12] B. C. Sawyer *et al.*, *Phys. Rev. Lett.* **98**, 253002 (2007).
- [13] B. L. Lev *et al.*, *Phys. Rev. A* **77**, 023402 (2008).
- [14] P. Domokos and H. Ritsch, *Phys. Rev. Lett.* **89**, 253003 (2002).
- [15] G. Morigi *et al.*, *Phys. Rev. Lett.* **99**, 073001 (2007).
- [16] A. André *et al.*, *Nature Phys.* **2**, 636 (2006).
- [17] J. T. Bahns *et al.*, *J. Chem. Phys.* **104**, 9689 (1996).
- [18] M. D. D. Rosa, *Eur. Phys. J. D* **31**, 395 (2004).
- [19] D. DeMille (private communication).
- [20] I. M. Hedgecock *et al.*, *Astron. Astrophys.* **304**, 667 (1995).
- [21] N. V. Dobrodey, *Astron. Astrophys.* **365**, 642 (2001).
- [22] T. Gustavsson *et al.*, *J. Mol. Spectrosc.* **145**, 56 (1991).
- [23] K. Kobayashi *et al.*, *J. Mol. Spectrosc.* **212**, 133 (2002).
- [24] S. R. Langhoff, *Astrophys. J.* **481**, 1007 (1997).
- [25] C. Lundevall, *J. Mol. Spectrosc.* **191**, 93 (1998).
- [26] K. Namiki *et al.*, *J. Mol. Spectrosc.* **191**, 176 (1998).
- [27] T. C. Steimle and W. Virgo, *Chem. Phys. Lett.* **381**, 30 (2003).
- [28] C. Amiot *et al.*, *J. Chem. Phys.* **102**, 4375 (1995).
- [29] T. Kuwamoto *et al.*, *Phys. Rev. A* **60**, R745 (1999).
- [30] D. Egorov *et al.*, *Phys. Rev. A* **66**, 043401 (2002).
- [31] H. J. Metcalf and P. van der Straten, *Laser Cooling and Trapping* (Springer, New York, 2001).
- [32] W. Virgo and T. C. Steimle, *Astrophys. J.* **628**, 567 (2005).
- [33] T. Mukaiyama *et al.*, *Phys. Rev. Lett.* **90**, 113002 (2003).
- [34] B. C. Sawyer *et al.*, *Phys. Rev. Lett.* **101**, 203203 (2008).